Investigation of the diurnal cycle of stratocumulus clouds at the northern coast of Chile

Westbrook[1]*, S., J. H. Schween*[1]*, and U. Löhnert*[1]

[1] *Institute for Geophysics and Meteorology, University of Cologne*

Earth – Evolution at the dry limit

DFG CRC1211, https://sfb1211.uni-koeln.de

1. Introduction

Marine stratocumulus clouds of the eastern Pacific play a crucial role for the Earth's energy and water cycles (Wood, 2012). Parts of these extensive clouds off the west coast of South America form the major source of water to the hyper-arid area at the northern coast of Chile.

- Within the Collaborative Research Center 'Earth-Evolution at the Dry Limit' three ground-based remote sensing instruments were installed at the airport of Iquique.
- We use the data of nearly one year in order to characterize the vertical structure of the clouds and their environment.
- Climate is dominated by high pressure system above southeast Pacific and low sea surface temperatures (SSTs) due to the cold Humboldt Current.

***Fig. 1**: Instrumentation at the airport of Iquique (20.5°S, 70.2°W, 56m AMSL). Instruments from left to right: cloud radar JOYRAD-94, wind lidar Halo Streamline (provided by the Finish Meteorological Institute (FMI)), microwave radiometer FOGHAT (AG Crewell, 2019).*

surface pressure, SSTs and IWV show distinct seasonal variation

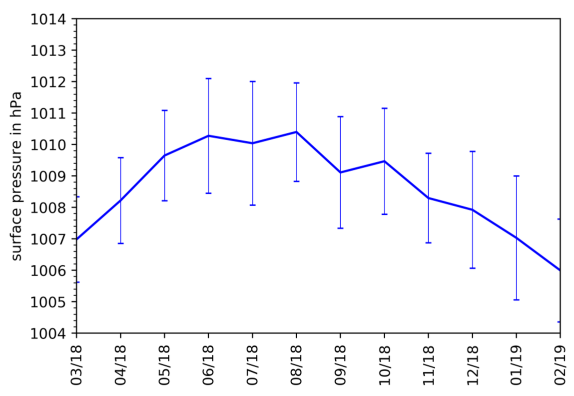

***Fig. 2**: Annual cycle of surface pressure (with standard deviations) for March 2018 – March 2019 measured by an integrated automatic weather station mounted on the microwave radiometer in Iquique.*

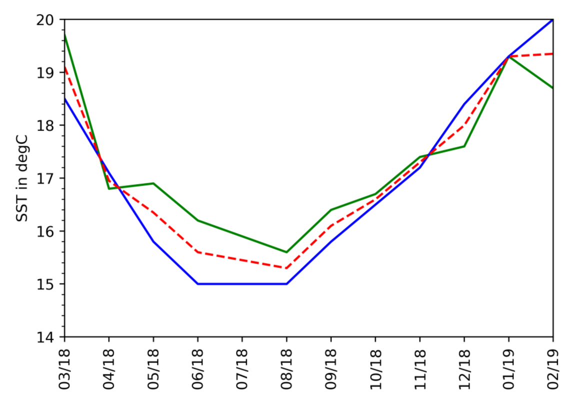

***Fig. 3**: Annual cycle of SSTs measured at the coasts of Arica (green) and Antofagasta (blue) by the Chilean Navy Hydrographic and Oceanographic Service (SHOA). The dashed line is the mean of both stations.*

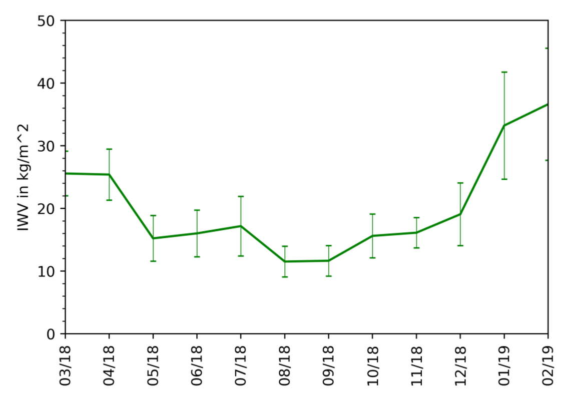

***Fig. 4**: Annual cycle of integrated water vapor (IWV) (with standard deviations) for March 2018 – March 2019 measured by the microwave radiometer in Iquique.*

2. Coastal cliff circulation

In order to be able to understand the diurnal cycle of the coastal clouds, wind lidar data is used to characterize the coastal circulation as a function of height. 30-minute means of horizontal wind speed and direction have been calculated. The mean values were then averaged on seasonal time scales.

<u>night / early morning</u>:

- weak winds (mean around 1m/s)
- SE winds near surface
- NW winds at top of marine boundary layer (MBL) (>1000m no signal due to clouds or too few aerosols)

<u>day / early evening</u>:

- stronger winds (max. mean around 7m/s)
- strong SW surface winds
- NE and E winds at top of MBL

→ land-sea-breeze circulation with superimposed S winds

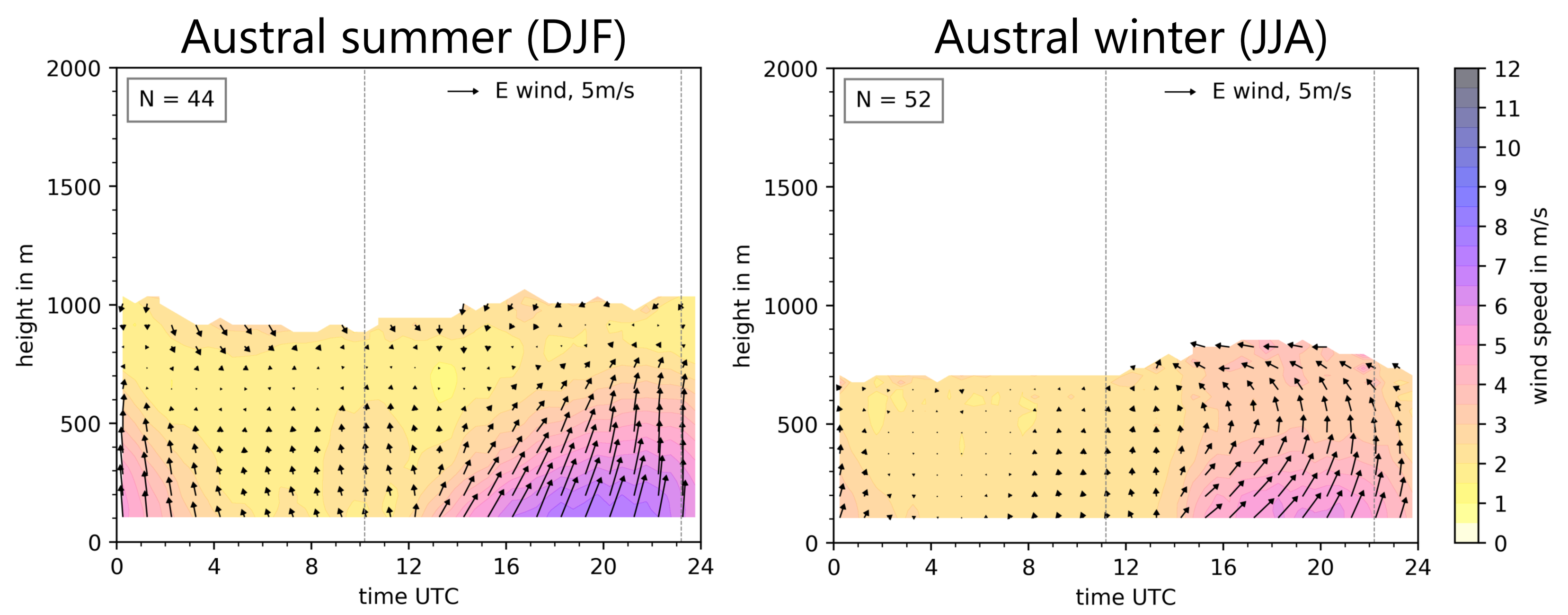

***Fig. 5**: Diurnal cycle of the averaged 30-minute mean values of horizontal wind speed (color scale) and direction (arrows) for austral summer (DJF) (left) and austral winter (JJA) (right). N gives the number of days that were available to calculate the seasonal mean values. Mean times of sunrise and sunset are marked by the vertical dashed lines (black).*

References:

AG Crewell, IGMK, 2019: **Iquique – CRC1211**, http://gop.meteo.uni-koeln.de/ag_crewell/doku.php?id=sites:iquique.

Illingworth, A., R. Hogan, E. O'Connor, D. Bouniol, M. Brooks, et al., 2007: **Cloudnet**, Bull. Amer. Meteor. Soc., 88, 883–898.

Manninen, A., T. Marke, M. Tuononen, and E. O'Connor, 2018: **Atmospheric Boundary Layer Classification With Doppler Lidar**, Journal of Geophysical Research: Atmospheres, 123 (15), 8172-8189.

SHOA, 2019: **Sea Surface Temperature (SST)**, https://www.shoa.cl/php/tsm.php?idioma=en.

Wood, R., 2012: **Stratocumulus Clouds**, Monthly Weather Review, 140, 2373-2432.

3. Diurnal cycle of cloud occurrence

The Cloudnet algorithm (Illingworth et al., 2007) was applied to the data to derive vertical cloud structure information. For each timestep it was investigated if cloud liquid droplets (also with drizzle) were detected.

- clouds more frequent in austral winter than in summer
- lowest clouds in austral winter
- max. cloud occurrence during night / early morning
- frequently no clouds in the afternoon

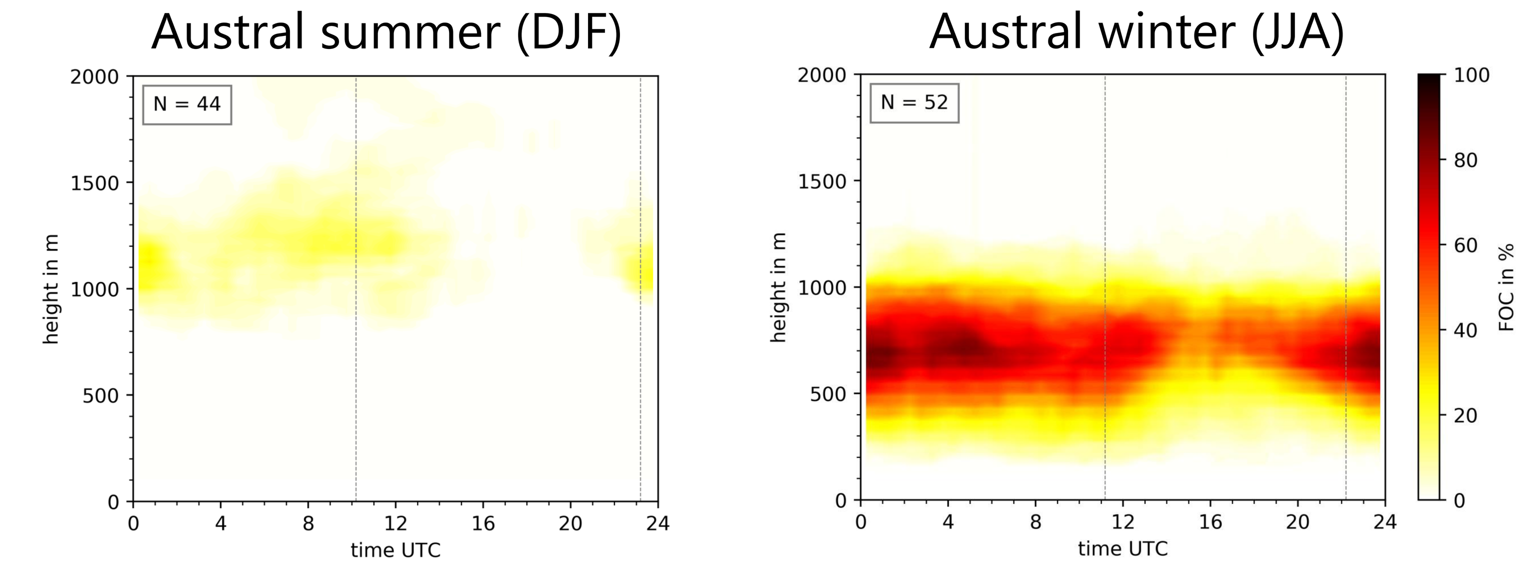

***Fig. 6**: Diurnal cycle of cloud occurrence below 2000m for austral summer (DJF) (left) and austral winter (JJA) (right). N gives the number of days that were available to calculate the frequency of occurrence (FOC) of cloud liquid droplets. Mean times of sunrise and sunset are marked by the vertical dashed lines (black).*

4. Atmospheric boundary layer classification

Following the method of Manninen et al. (2018) Doppler lidar data is used to identify sources of turbulent mixing.

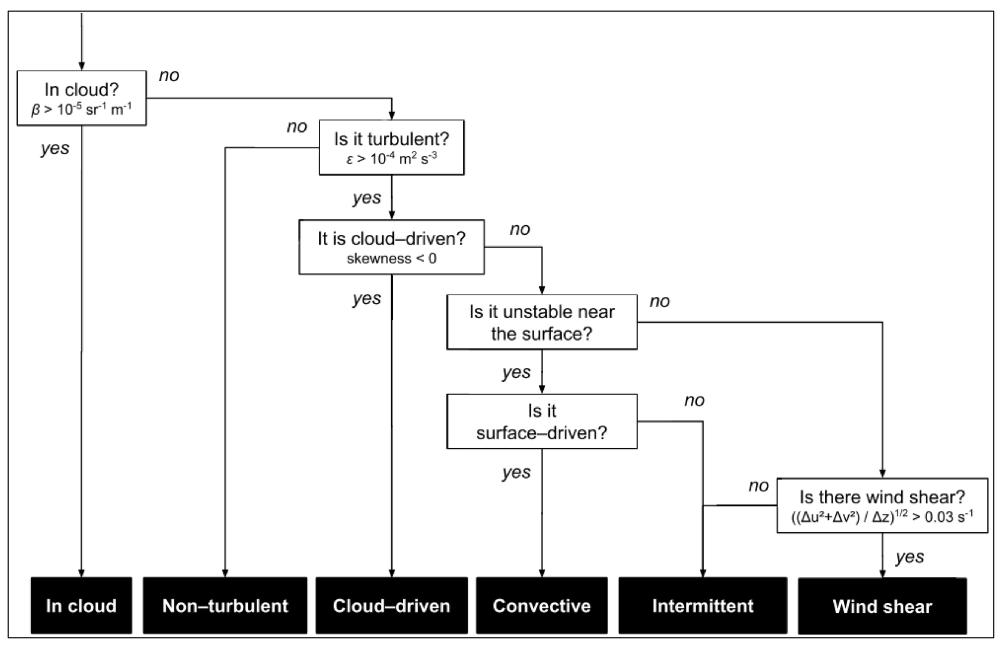

***Fig. 7**: Schematic of the atmospheric boundary layer decision tree used to identify the source of turbulent mixing (Manninen et al., 2018). First, pixels are identified as being located in cloud or not. After this, turbulent pixels are separated from non-turbulent (by comparing the dissipation rate of turbulent kinetic energy ε to a certain threshold), and cloud-driven pixels are identified. The classification of other turbulent pixels depends on the atmospheric stability close to the surface, whether they are in contact with the surface, and also whether wind shear is present. Unassigned pixels are labeled as intermittent.*

<u>Results</u>

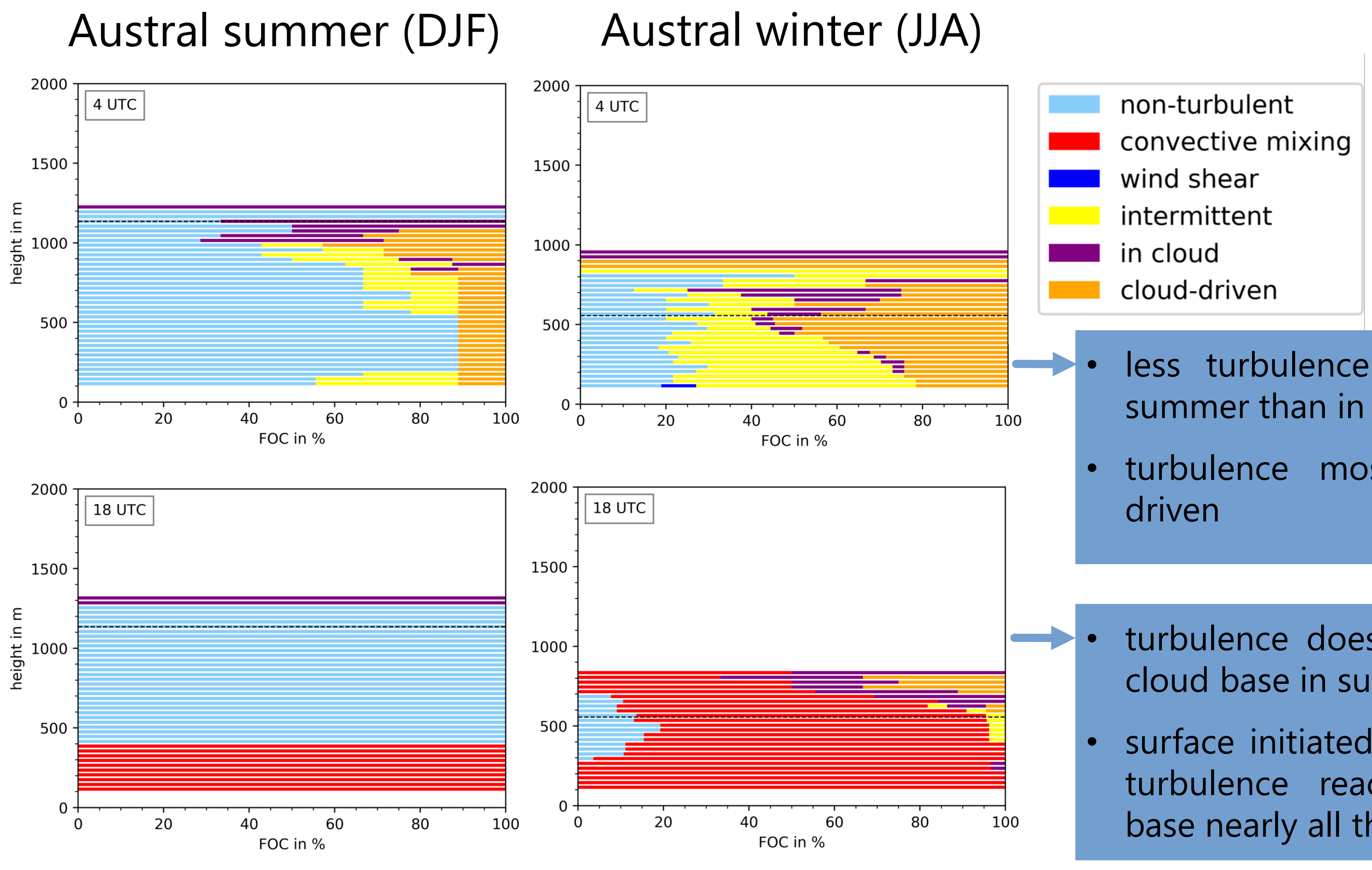

- less turbulence in austral summer than in winter
- turbulence mostly cloud-driven

- turbulence does not reach cloud base in summer
- surface initiated convective turbulence reaches cloud base nearly all the time

***Fig. 8**: FOC of the different ABL classes for austral summer (DJF) (left) and austral winter (JJA) (right) during night at 4 UTC (top) and day at 18 UTC (bottom). In order to understand the cloud lifetime cycle only cloudy cases have been considered (during summer only few cases are considered since clouds are less frequent than in winter (see fig. 6)). The horizontal dashed line marks the seasonal mean cloud base height.*

seasonal and diurnal differences in mixing of ABL → different nature of ABL clouds!

5. Outlook

Describe full circulation patterns (also above 1.5 km) by using realistic large eddy simulations nudged with CRC1211 observations.